

A Comparison of Stress Corrosion Cracking Susceptibility in Additively-Manufactured and Wrought Materials for Aerospace and Biomedical Applications

Michael Roach¹, R. Scott Williamson¹, Jonathan Pegues^{2,3}, Nima Shamsaei^{2,3,*}

¹*Department of Biomedical Materials Science, University of Mississippi Medical Center,
Jackson, MS 39216*

²*Department of Mechanical Engineering, Auburn University, Auburn, AL 36849*

³*National Center for Additive Manufacturing Excellence (NCAME), Auburn University, Auburn,
AL 36849*

*Corresponding author: shamsaei@auburn.edu

Abstract

Additive manufacturing (AM) is becoming an increasingly popular method in both aerospace and biomedical industries. Titanium alloys are increasingly common in additive manufactured applications due to their excellent strength to weight ratio and biocompatibility. Traditional wrought Ti-6Al-4V alloys show little sensitivity to stress corrosion cracking (SCC) when subjected to in-vitro conditions. In AM applications the alloy powder is often sifted and reused multiple times which often results in a degradation of the powder's shape. Recent studies have also shown that the oxygen content of additive powders increases with repeated powder use which may increase the susceptibility of the resulting parts to SCC. This research compares the microstructural characteristics and tensile SCC behavior of AM Ti-6Al-4V parts fabricated from new and recycled powder in distilled H₂O, salt water, and Ringers solution. Additionally, the effect of surface finish is investigated for each microstructure comparing the as-built surfaces to machined and polished surfaces.

Keywords: Stress corrosion cracking, environmentally assisted cracking, titanium alloy, tensile properties

Introduction

As additively manufacturing becomes a more viable option for fabrication of structural components in a wide range of biomedical and aerospace applications there is a critical need to understand the failure mechanisms related to these specific applications. As a result, numerous studies have recently been published comparing mechanical behavior of additively manufactured (AM) titanium alloy parts to their wrought material counterparts [1]–[13]. Despite this recent surge

of research the effect of environmentally assisted cracking (EAC) and its effect of stress corrosion cracking (SCC) has not been well represented for additive manufactured (AM) materials.

Titanium alloys such as Ti-6Al-4V are common in both biomedical and aerospace industries due to their high strength to weight ratio, biocompatibility, and excellent corrosion resistance. In both of these industries parts are often subjected to harsh environments that may lead to an increased susceptibility to SCC [14], [15]. While the EAC failure mechanisms are well reported for wrought Ti-6Al-4V and believed to be of relatively low risk, however, the unique microstructure, equilibrium phases, and high surface roughness associated with AM parts could lead to an increased risk of SCC compared to its wrought counterpart. Recent studies have also shown that the oxygen content of additive powders increases with repeated powder use which may increase the susceptibility of the resulting parts to SCC [16], [17].

The purpose of the present research was to compare the ASTM G129 slow strain rate (SSR) SCC susceptibility of Ti-6Al-4V samples fabricated using laser powder bed fusion (LPBF) technology, to those fabricated using traditional machined wrought samples from the same alloy. The ductility of AM Ti-6Al-4V samples were compared to their wrought counterparts in distilled water, Ringer's, and 3.5% NaCl electrolytes. Additionally, the SCC response of titanium AM samples fabricated from the virgin and reconditioned powders were compared for both as-built and machined conditions.

Experimental Set-up

Test coupons were designed accordance to ASTM G129 [18] with the dimensions shown in Figure 1. Grip ends were threaded in order to submerge the test coupons in the desired solution during testing. Two solutions, Ringer's and 3.5% NaCl, were selected to test for stress corrosion cracking susceptibility compared to distilled H₂O as the control solution. Ringer's solution is often used in testing to simulate physiological conditions. Additionally, a 3.5% NaCl solution is often used in testing to simulate a seawater environment. For the Ringer's solution, a test temperature of 37°C was chosen as a representative in-vivo condition for surgical implants while room temperature (23°C) was selected for testing in the 3.5% NaCl solution. For the control solution, a test temperature of 37°C was used.

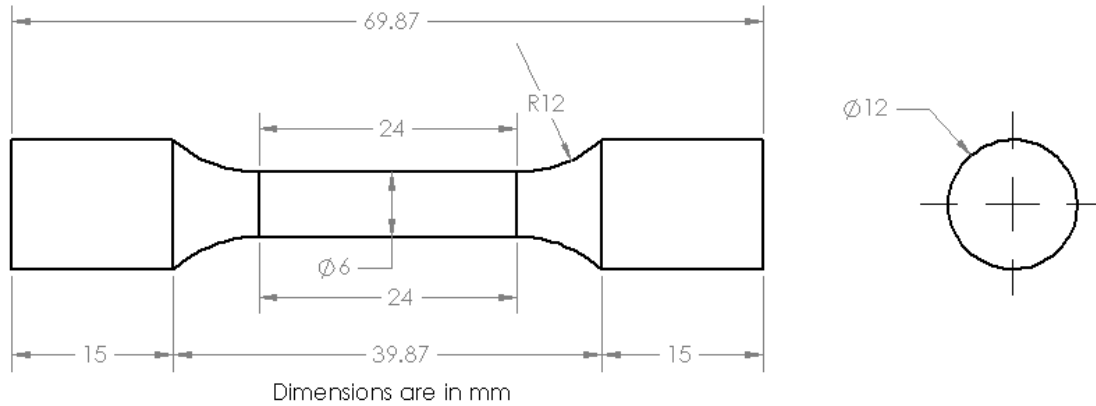


Figure 1: Specimen geometry used for slow strain rate testing.

Slow strain rate tensile tests were performed on an MTS load frame with a 100 kN capacity. A displacement stroke rate of 2.5×10^{-5} mm/s was chosen which results in an approximate strain rate of 1×10^{-6} s⁻¹. Test specimens were completely submerged in the test solution and the temperature was monitored and controlled using a Digi-Sense temperature controller. Figure 2 gives a representation of the test setup used for this study. All samples were tested until failure, after which, a measuring microscope was used to determine the elongation to failure and reduction of area (RoA). Fracture surfaces were then examined with both a Keyence digital microscope and a Zeiss scanning electron microscope (SEM). Ratios between the control environment and the harsh environment were calculated by dividing the mean values of samples in harsh environments by the mean values of the samples in the control (distilled H₂O). ASTM G129 [18] states that ratios that are less than unity are considered to be susceptible to SCC. For this study a more strict definition of ratios falling below 0.9, which has been used in previous studies [14], is considered to be susceptible to SCC.



Figure 2: Test set up showing specimen submerged in solution during testing.

Results

The elongation to failure, reduction of area, and time to failure were averaged for each condition and are listed in Table 1. The elongation and reduction of area are significantly lower than the wrought conditions which is consistent with literature on L-PBF Ti-6Al-4V [5], [13], [19]. The low ductility of AM L-PBF Ti-6Al-4V is attributed to the fine acicular martensitic microstructure as a result of the high cooling rate during fabrication. Rapid solidification in the fabrication process does not allow the diffusive α transformation to occur, thus, the β phase transforms to the α' phase through the non-diffusive martensitic transformation [20]. Additionally, the elongation to failure for all conditions reported in this study is much lower than the required 10% elongation to failure required by ASTM F2924 [21] for AM Ti-6Al-4V.

Table 1: Slow strain rate results for each condition.

Condition	Powder	Solution	Temp. (°C)	Elongation (%)	RoA (%)	Time (Hrs)
As-Built	New	H ₂ O	37	6.27	28.2	41.29
As-Built	Reused	H ₂ O	37	6.10	25.2	40.15

As-Built	New	Ringers	37	5.58	23.3	40.79
As-Built	Reused	Ringers	37	5.31	25.2	39.93
As-Built	New	3.5% NaCl	23	5.30	21.7	38.33
As-Built	Reused	3.5% NaCl	23	4.97	23.9	38.16
Machined	New	H ₂ O	37	5.92	31.9	39.12
Machined	New	Ringers	37	5.83	34.0	41.01
Wrought [1]	NA	H ₂ O	37	21.8	53.7	NA
Wrought [1]	NA	Ringers	37	20.5	53.3	NA

A visual representation of the slow strain rate tensile properties for each condition is shown using a box plot in Figure 3. The dotted lines on each box plot represents the lower range of the control solution with the black line representing the machined control condition and the red line representing the as-built control condition. The elongation to failure was mostly similar for all conditions and solutions with only the 3.5% NaCl solution showing significant decreases. There was a slight decrease in elongation to failure for samples in Ringer's, however, the difference is not significant. A similar trend was observed for the reduction of area (RoA) with Ringer's and 3.5% NaCl showing slightly lower RoA. Interestingly, while no difference was observed between as-built and machined specimens in elongation to failure, as-built specimens did show consistent decreases in RoA compared to machined specimens. Finally, there was no significant differences in the time to failure for all conditions.

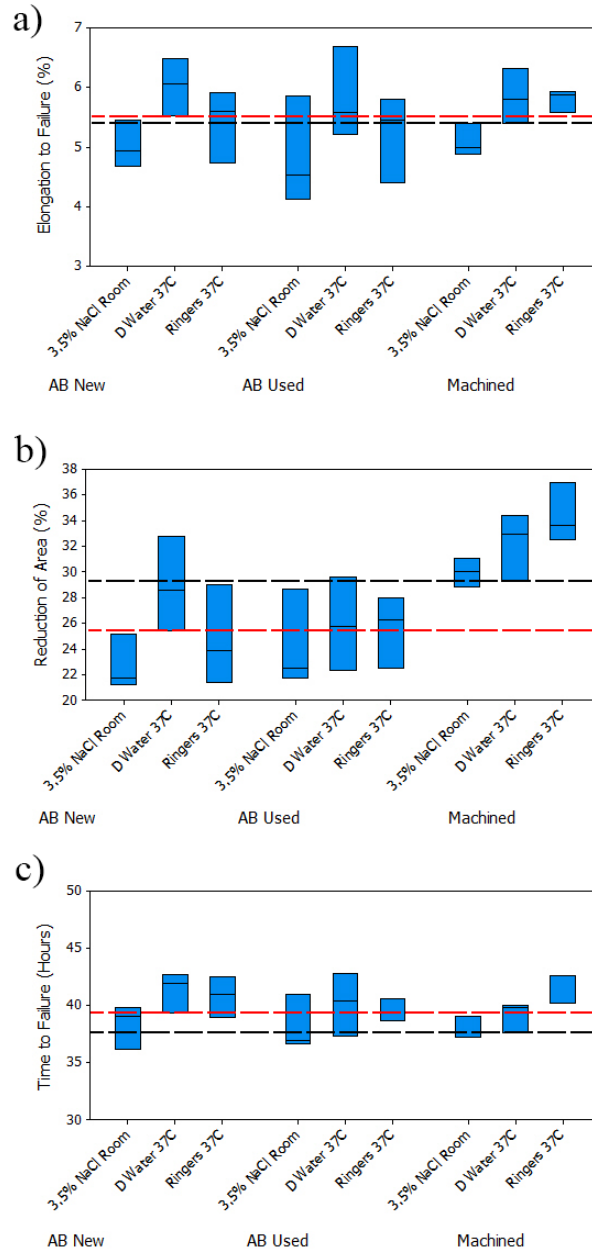


Figure 3: Box plots showing the spread in data for all conditions.

Evaluation of environmentally assisted cracking for slow strain rate testing, according to ASTM G129 [18], is carried out by comparing the SSR ratios to the control environment with ratios reaching unity being considered not susceptible to SCC. Decreasing SSR ratios are considered to show increasing susceptibility to SCC. In general, for biomedical applications, ratios that are lower than 0.9 are considered to show some susceptibility to SCC [14]. Table 2 lists the elongation ratio (RE), the reduction of area ratio (RRA), and time to failure ratio (RTTF) calculated

for each condition. The control for all machined specimens is the machined new powder in distilled H₂O while the control for all as-built conditions was the as-built new powder in distilled H₂O.

Table 2: Calculated ratios for each condition, * represents control for surface condition.

Condition	Powder	Solution	Temp. (°C)	RE	RRA	RTTF
*Machined	New	H ₂ O	37	1.00	1.00	1.00
Machined	New	Ringers	37	0.98	1.07	1.05
Machined	New	3.5% NaCl	23	0.87	0.93	0.97
*As-Built	New	H ₂ O	37	1.00	1.00	1.00
As-Built	Reused	H ₂ O	37	0.97	0.89	0.97
As-Built	New	Ringers	37	0.89	0.83	0.99
As-Built	Reused	Ringers	37	0.85	0.90	0.97
As-Built	New	3.5% NaCl	23	0.84	0.77	0.93
As-Built	Reused	3.5% NaCl	23	0.79	0.85	0.92

Comparing the ratios for each condition given in Table 2, there are several areas that indicate susceptibility to SCC for L-PBF Ti-6Al-4V. For the machined conditions there is a decrease in the elongation to failure in the 3.5% NaCl solution, however, the reduction of area is only slightly reduced. The most notable observation is the significant decrease in ductility for all as-built conditions. While the elongation to failure ratio was not significantly reduced for distilled H₂O fabricated from both new and reused powder, all other as-built geometries showed significant (< 0.9) decreases in RE. Additionally, the RRA was also considered to be significant (< 0.9) for all as-built surfaces outside of the control condition. This indicates that the high roughness associated with the as-built geometries could potentially increase the susceptibility of EAC for AM Ti-6Al-4V. Additionally, all 3.5% NaCl environments showed some loss in ductility compared to the control environment with significantly low RRA (≤ 0.75) for the as-built conditions. The reduced ductility for the Ringer's and 3.5% NaCl conditions suggests that AM Ti-6Al-4V parts could potentially show an increased risk of EAC in harsh environments in the presence of high surface roughness. Additionally, another observation than can be made from Table 2 is the further decrease in ductility for all 3.5% NaCl solutions. More tests for specimens in 3.5% NaCl at 37° C and distilled H₂O at 23°C are necessary to ensure the difference in testing temperature is not playing some role in the SCC behavior.

Fractography analysis revealed a change in crack behavior between the control and 3.5% NaCl solutions while the Ringer's solution was mostly similar to the control. Representative fracture surfaces for each condition are shown in Figure 4. For the control condition in Fig. 4(a) the crack propagation appears to be deflect along prior β grains as indicated by the deep valleys. Closer inspection of these valleys to the right of Fig. 4(a) reveals that these appear to be ends of

prior β grains being pulled completely from the surface. This type of crack propagation results in multiple crack deflections leading to a tortuous fracture surface. Similarly, the fracture surface of the representative Ringer's solution in Fig. 4(b) shows multiple crack deflections along the prior β grains resulting in a tortuous fracture surface. Conversely, the 3.5% NaCl fracture surface shows a less tortuous crack path which is attributed to very little failure along prior β grains. This type of crack propagation consists of less crack deflection ultimately leading to the lower ductility in the 3.5% NaCl specimens.

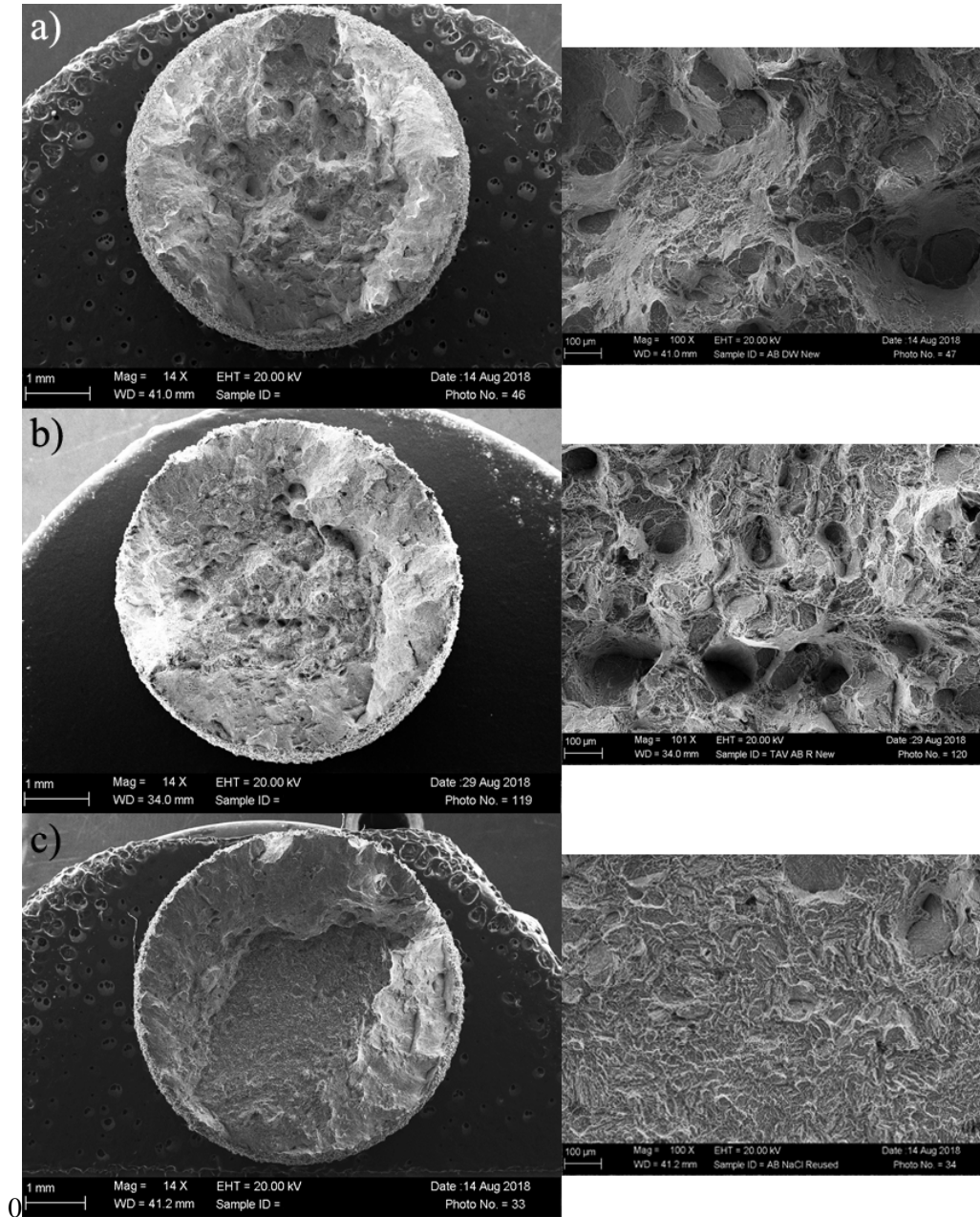


Figure 4: Fracture surfaces of the as-built condition in a) distilled H₂O, b) Ringers, and c) 3.5% NaCl.

Conclusions

The results presented in this study indicate that additive manufactured Ti-6Al-4V may be susceptible to stress corrosion cracking. A decrease in elongation to failure was observed for a solution of machined 3.5% NaCl while the machined Ringer's solution showed similar elongation to failure as the control in the machined condition. However, all samples in the as-built condition showed significant reduction of area ratios (< 0.9) compared to the as-built control. The reduction in elongation to failure in the as-built conditions was observable but less severe than the reduction of area. This significant loss in ductility for the as-built specimens in Ringer's and 3.5% NaCl compared to distilled H₂O in the as-built condition indicate that the presence of the rough surface may increase the susceptibility of AM Ti-6Al-4V to SCC. These results, while preliminary, do indicate that stress corrosion cracking could be of concern for AM Ti-6Al-4V in the presence of harsh environments. Further tests are in progress to determine the effect of testing temperature in relation to the test solution. Additionally, further in-depth studies are needed to fully assess the effect of harsh environments on AM parts.

Acknowledgements

Partial funding for this work was provided by the National Science Foundation under Grant No. 1657195. Supports from the Naval Air Systems Command (NAVAIR) is also greatly appreciated.

References

- [1] B. E. Carroll, T. A. Palmer, and A. M. Beese, "Anisotropic tensile behavior of Ti-6Al-4V components fabricated with directed energy deposition additive manufacturing," *Acta Mater.*, vol. 87, no. Supplement C, pp. 309–320, Apr. 2015.
- [2] A. J. Sterling, B. Torries, N. Shamsaei, S. M. Thompson, and D. W. Seely, "Fatigue behavior and failure mechanisms of direct laser deposited Ti-6Al-4V," *Mater. Sci. Eng. A*, vol. 655, pp. 100–112, Feb. 2016.
- [3] K. S. Chan, M. Koike, R. L. Mason, and T. Okabe, "Fatigue Life of Titanium Alloys Fabricated by Additive Layer Manufacturing Techniques for Dental Implants," *Metall. Mater. Trans. A*, vol. 44, no. 2, pp. 1010–1022, Feb. 2013.
- [4] P. Edwards and M. Ramulu, "Fatigue performance evaluation of selective laser melted Ti-6Al-4V," *Mater. Sci. Eng. A*, vol. 598, pp. 327–337, Mar. 2014.
- [5] L. Facchini, E. Magalini, P. Robotti, A. Molinari, S. Höges, and K. Wissenbach, "Ductility of a Ti-6Al-4V alloy produced by selective laser melting of prealloyed powders," *Rapid Prototyp. J.*, vol. 16, no. 6, pp. 450–459, Oct. 2010.
- [6] D. A. Hollander *et al.*, "Structural, mechanical and in vitro characterization of individually structured Ti-6Al-4V produced by direct laser forming," *Biomaterials*, vol. 27, no. 7, pp. 955–963, Mar. 2006.
- [7] M. Kahlin, H. Ansell, and J. J. Moverare, "Fatigue behaviour of additive manufactured Ti6Al4V, with as-built surfaces, exposed to variable amplitude loading," *Int. J. Fatigue*, vol. 103, pp. 353–362, Oct. 2017.

- [8] S. Leuders *et al.*, “On the mechanical behaviour of titanium alloy TiAl6V4 manufactured by selective laser melting: Fatigue resistance and crack growth performance,” *Int. J. Fatigue*, vol. 48, pp. 300–307, Mar. 2013.
- [9] H. Matsumoto *et al.*, “Room-temperature ductility of Ti–6Al–4V alloy with α' martensite microstructure,” *Mater. Sci. Eng. A*, vol. 528, no. 3, pp. 1512–1520, Jan. 2011.
- [10] L. E. Murr *et al.*, “Microstructures and mechanical properties of electron beam-rapid manufactured Ti–6Al–4V biomedical prototypes compared to wrought Ti–6Al–4V,” *Mater. Charact.*, vol. 60, no. 2, pp. 96–105, Feb. 2009.
- [11] R. K. Nalla, R. O. Ritchie, B. L. Boyce, J. P. Campbell, and J. O. Peters, “Influence of microstructure on high-cycle fatigue of Ti-6Al-4V: Bimodal vs. lamellar structures,” *Metall. Mater. Trans. A*, vol. 33, no. 3, pp. 899–918, Mar. 2002.
- [12] J. Pegues, M. Roach, R. Williamson, and N. Shamsaei, “Surface Roughness Effects on the Fatigue Strength of Additively Manufactured Ti-6Al-4V,” *Int. J. Fatigue*, Accepted 2018.
- [13] W. Xu *et al.*, “Additive manufacturing of strong and ductile Ti–6Al–4V by selective laser melting via in situ martensite decomposition,” *Acta Mater.*, vol. 85, no. Supplement C, pp. 74–84, Feb. 2015.
- [14] R. S. Williamson, M. D. Roach, and L. D. Zardiackas, “Comparison of Stress Corrosion Cracking of Ti-15Mo, Ti-6Al-7Nb, Ti-6Al-4V, and CP Ti,” *ASTM Int. STP*, vol. 1471, pp. 166–177, 2004.
- [15] M. D. Roach, R. S. Williamson, and L. D. Zardiackas, “Comparison of the Corrosion Fatigue Characteristics of CP Ti-Grade 4, Ti-6Al-4V ELI, Ti-6Al-7Nb, and Ti-15Mo,” *ASTM Int.*, Jan. 2006.
- [16] J. C. Fox, S. P. Moylan, and B. M. Lane, “Effect of Process Parameters on the Surface Roughness of Overhanging Structures in Laser Powder Bed Fusion Additive Manufacturing,” *Procedia CIRP*, vol. 45, pp. 131–134, Jan. 2016.
- [17] Y. Sun, M. Aindow, and R. J. Hebert, “The effect of recycling on the oxygen distribution in Ti-6Al-4V powder for additive manufacturing,” *Mater. High Temp.*, vol. 35, no. 1–3, pp. 217–224, May 2018.
- [18] “Standard Practice for Slow Strain Rate Testing to Evaluate the Susceptibility of Metallic Materials to Environmentally Assisted Cracking,” 2013.
- [19] J. Pegues *et al.*, “Effect of Process Parameter Variation on Microstructure and Mechanical Properties of Additively Manufactured Ti-6Al-4V,” *Solid Free. Fabr. 2017 Proc. 28th Annu. Int.*, p. 14, 2017.
- [20] J. Yang, H. Yu, J. Yin, M. Gao, Z. Wang, and X. Zeng, “Formation and control of martensite in Ti-6Al-4V alloy produced by selective laser melting,” *Mater. Des.*, vol. 108, pp. 308–318, Oct. 2016.
- [21] “Standard Specification for Additive Manufacturing Titanium-6 Aluminum-4 Vanadium with Powder Bed Fusion,” 14.